OPEN

Distribution and Repeatability of Corneal Astigmatism Measurements (Magnitude and Axis) Evaluated With Color Light Emitting Diode Reflection Topography

Anastasios John Kanellopoulos, MD,† and George Asimellis, PhD**

Purpose: To evaluate and investigate the distribution and repeatability of anterior corneal surface astigmatism measurements (axis and magnitude) using a novel corneal topographer.

Methods: Anterior corneal surface astigmatism was investigated in a total of 195 eyes using a novel multicolored spot reflection topographer (Cassini; i-Optics). Two patient groups were studied, a younger-age group A and an older-age group B. Three consecutive acquisitions were obtained from each eye. The repeatability of measurement was assessed using Bland–Altman plot analysis and is reported as the coefficient of repeatability.

Results: Group A (average age 34.3 years) had on average with-the-rule astigmatism, whereas the older-age group B (average age 72.3 years) had on average against-the-rule astigmatism. Average astigmatism magnitude measurement repeatability in group A was 0.4 diopters (D) and in group B 0.4 D. Average astigmatism axis measurement repeatability in group A was 5.4 degrees and in group B 5.5 degrees. The axis measurement repeatability improved with increasing magnitude of astigmatism: in the subgroups with astigmatism between 3.0 and 6.0 D, the axis repeatability was 1.4 degrees (group A) and 1.2 degrees (group B), whereas in the subgroups with astigmatism larger than 6.0 D, the repeatability was 1.1 and 0.6 degrees, respectively.

Conclusions: This novel corneal topography device seems to offer high precision in reporting corneal astigmatism. This study reaffirms the established trend of a corneal astigmatism shift from an average "with-the-rule" to "against-the-rule" with aging.

Received for publication November 14, 2014; revision received January 12, 2015; accepted April 5, 2015. Published online ahead of print June 9, 2015.

From the *Laservision.gr Clinical and Research Eye Institute, Athens, Greece; and †Department of Ophthalmology, New York University Medical School, New York, NY.

A. J. Kanellopoulos is a consultant to and holds advisory positions in Alcon/WaveLight, Allergan, Avedro, i-Optics, and KeraMed. The other author has no funding or conflicts of interest to disclose.

Reprints: Anastasios John Kanellopoulos, MD, NYU Medical School, Department of Ophthalmology, New York, NY, Laservision.gr Clinical and Research Eye Institute, 17 Tsocha St, Athens 11521, Greece (e-mail: ajk@brilliantvision.com).

Key Words: color LED reflection topography, axis and magnitude of astigmatism, Cassini, astigmatism shift with aging, astigmatism repeatability

(*Cornea* 2015;34:937–944)

The anterior corneal surface offers noncontact imaging accessibility. In addition, it is the major refractive element of the eye, corresponding to more than two-thirds [48 diopters (D)] of the total ocular refractive power. Thus, the anterior corneal surface has the potential to effect a very large change in the total ocular power as a result of a relatively small change in its surface curvature.

Evaluation of the anterior corneal surface may be performed by a multitude of devices. Placido ring projection is a long-standing and established modality used for the topographic analysis of the anterior cornea. Aiming to overcome the limitations of this technique,[1] other systems have been proposed.[2,3] The "VU Topographer" (Vrije Universiteit Medical Center, Amsterdam, the Netherlands)[2] used a color-coded chess-like square pattern,[4] whose crossing points were used to eliminate source image mismatch, enabling one-to-one correspondence. This early corneal topographer was found to be, in principle, superior in reconstructing nonrotationally symmetric features of the anterior corneal surface.[5]

The Cassini (i-Optics, the Hague, the Netherlands) is a novel topographer using a nonrotationally symmetric projection pattern emitting from up to 700 distinct light emitting diode (LED) color (red, yellow, and green) spots. The algorithm analyzes the captured pattern of the corresponding individual reflected images and provides elevation-based corneal topography analysis.

Because of the novelty of this device, clinical validation and performance assessment are yet to be reported. We have recently published early results using this new topographer in cases of central corneal scar imaging[6] and forme fruste keratoconus.[7] To the best of our knowledge, there are as yet no other publications in the peer-reviewed literature investigating its clinical applicability. The purpose of this work was to investigate the repeatability of astigmatism measurements (magnitude and axis) by this newly introduced multicolored spot reflection corneal topographer.

MATERIALS AND METHODS

This observational prospective longitudinal study received approval by the Ethics Committee of the Laservision.gr Clinical

and Research Eye Institute and adhered to the tenets of the Declaration of Helsinki. Informed written consent was obtained from each subject at the time of the first clinical visit.

Inclusion Criteria

We evaluated healthy unoperated eyes of patients presenting to our clinic for a scheduled visit. We routinely screen with the Cassini for corneal evaluation of all refractive surgery candidates and all candidates for cataract surgery; this was the data pool from which the 2 studied groups derived. Exclusion criteria were current or past ocular pathology other than a refractive error or cataract condition, previous ocular surgery, epithelial defects, and present irritation or dry eye disorder; all conditions were confirmed by a complete ophthalmologic evaluation. From each patient, 1 eye, chosen randomly, was included in the study. The younger-age group A consisted of patients without cataract, and the older-age group B consisted of presurgery cataract patients, with a minimum of classification I on the Lens Opacity Classification System III.[8,9]

Instrumentation

The device used in this study was the Cassini (i-Optics), a multicolored LED spot reflection corneal topographer running on software version 2.0 (updated July, 2014). The image of an actual "color pattern" projected on the cornea is provided in Figure 1A; Figure 1B illustrates the 7 distinct "areas" of points to emphasize the nonsymmetric nature of the projected array pattern.

The system report provides anterior surface topography maps, including axial (Fig. 2A) and tangential curvature, refractive power, and elevation maps (Fig. 2B), all calculated over an 8.5-mm diameter corneal area. The system report also provides values for steep and flat keratometry (in D), axis orientation (in degrees), and related astigmatism (D). In addition, the system calculates 4 topographic indices relating to surface asphericity and 2 keratoconus indices, the surface regularity index and the surface asymmetry index.[10]

Data Collection and Analysis

Data were included in the study if the acquisition had at least 75% coverage, as reported by the quality factor. Three successive acquisitions were performed in each case (eye). The astigmatism magnitude was provided by the difference between the steep meridian minus the flat meridian keratometry, expressed in D; the axis of astigmatism was provided by the steep meridian orientation, expressed in degrees. The notation of 0 and 180 degree meridians for the axis presented a potential problem in the analysis. The value of 180 degrees was added to or subtracted from the axis numeric value, if within the set of 3 axis values (for the same eye) any of the value(s) was close to 180 degrees while the other(s) was close to 0 degree.

To assess measurement repeatability in each studied parameter (magnitude and axis), we constructed Bland–Altman plots, which depict data points consisting of the difference between these 3 values per case (vertical axis) versus the averages of the same values (horizontal axis). The plots also depict the upper limit of detection (ULA) line, provided by the mean $+2 \times$ SD, and the lower limit of detection (LLA) line, provided by the mean $-2 \times$ SD. The coefficient of repeatability, defined as $2 \times$ SD, was the metric used in this study to report the repeatability of measurement. Based on the above, the repeatability of measurement derives from the separation of either the ULA or the LLA lines from the mean line in each respective Bland–Altman plot, and is, by definition, positive.

Within both groups, we formed 4 subgroups based on the astigmatism magnitude: subgroups with astigmatism between 0.0 and 1.0 D; between 1.0 and 3.0 D; between 3.0 and 6.0 D; and subgroups with astigmatism larger than 6.0 D.

Descriptive statistics, linear regression, and Bland–Altman analysis were performed by Minitab version 16.2.3 (Minitab Ltd, Coventry, United Kingdom) and Microsoft Excel 13 (Microsoft Corp, Redmond, WA). Data are reported in the form of average ± SD (minimum to maximum).

RESULTS

There were 139 eyes included in group A, belonging to 79 male and 60 female patients. The mean subject age at the

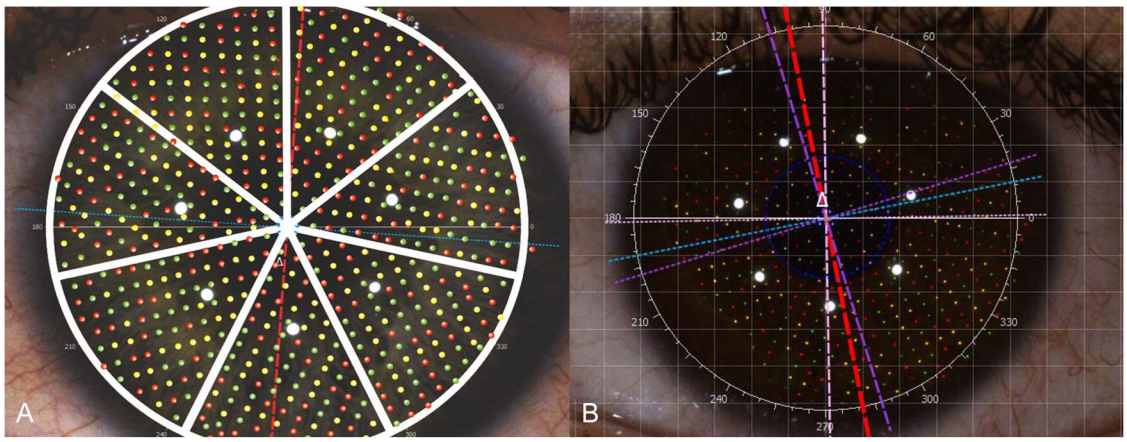

FIGURE 1. A, Illustration of the actual "color pattern" projected on the cornea. B, The 7 distinct "areas" of points are highlighted to illustrate the nonsymmetric pattern of the projected array.

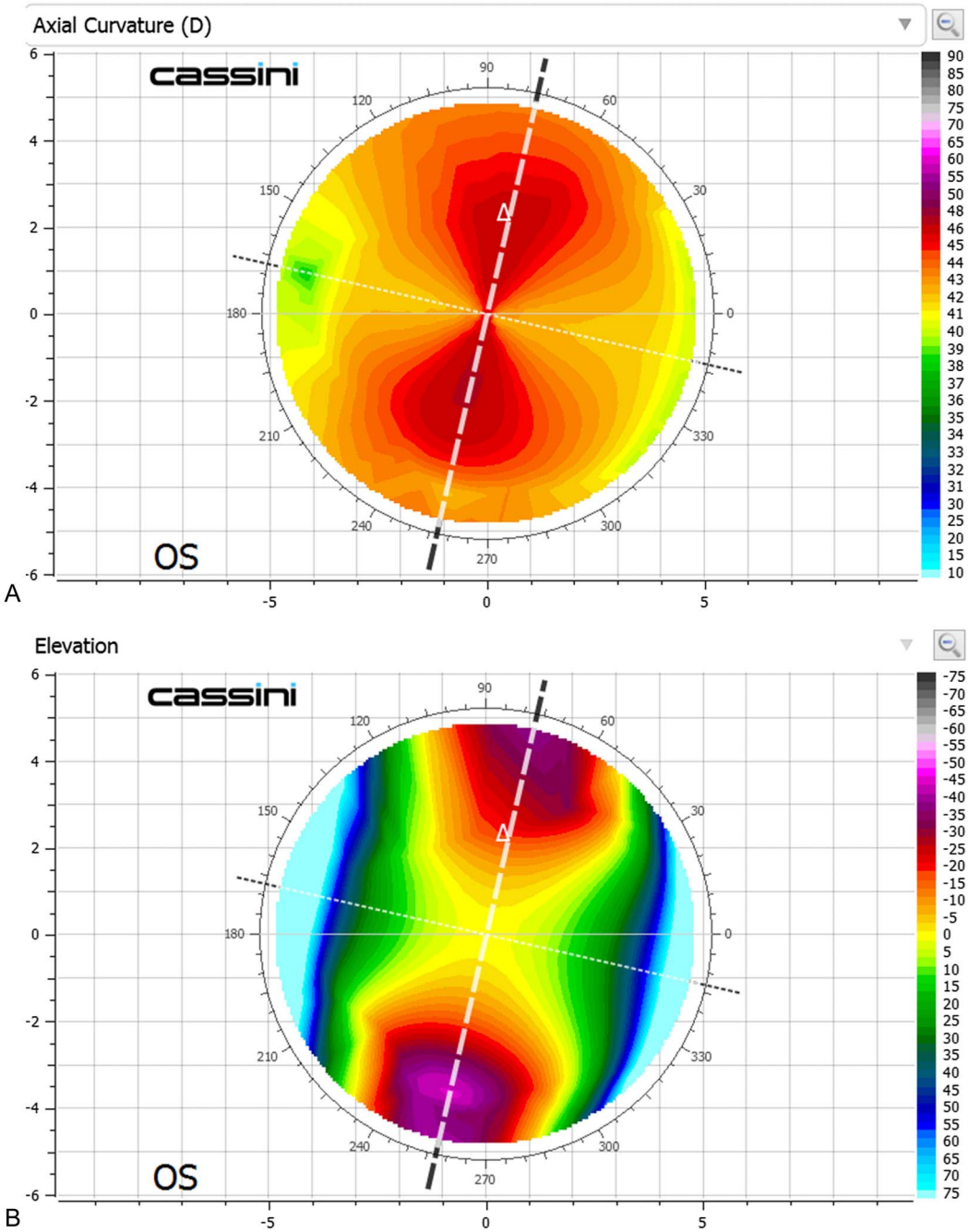

FIGURE 2. Topography data provided by the Cassini in the form of an axial curvature map (A) (color scale in D) and elevation map (B) (color scale in micrometers).

time of examination was 34.3 ± 14.5 years (16–59). The astigmatism magnitude was 1.6 ± 1.4 D (0.0–9.0). The average axis was 94.7 ± 27.2 degrees (0.5–179.8), considered as with-the-rule because 73.6% of the cases had an axis between 80 and 110 degrees.

Group B consisted of 56 eyes, belonging to 27 male and 29 female patients, with a mean age of 72.3 ± 5.9 (60–87) years. The astigmatism magnitude in this precataract group B was 1.3 ± 1.0 D (0.0–4.4). The average axis was 141.3 ± 57.9 degrees (0.3–179.6), considered as against-the-rule, because in 60.1% of the cases, the axis was between 0 and 30 degrees or 150 and 180 degrees.

Figure 3 presents astigmatism magnitude Bland–Altman plots. In group A (Fig. 3A), the coefficient of repeatability (illustrated as the separation of the ULA/LLA line(s) from the mean difference line) was 0.4 D. In group B (Fig. 3B), the coefficient of repeatability was 0.4 D.

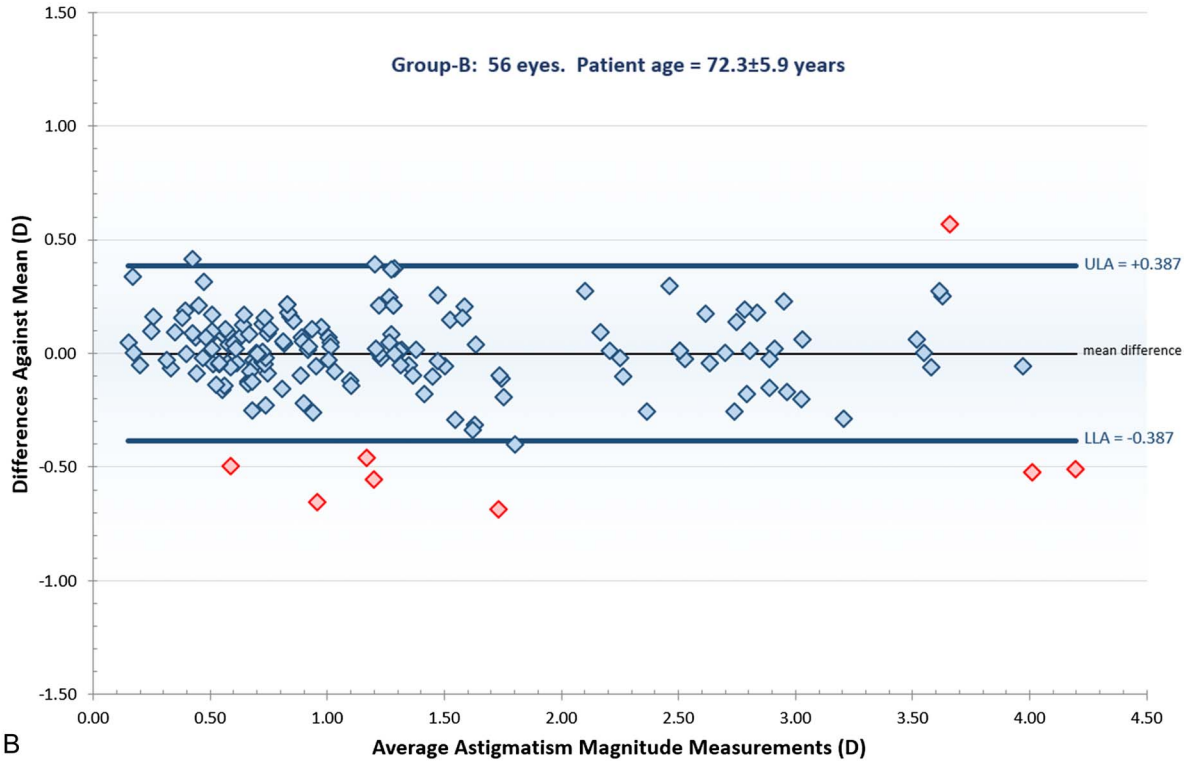

FIGURE 3. Bland–Altman plots illustrating the difference against means versus average astigmatism magnitude (reported in D) measurements. The ULA is defined as mean +2 × SD. The LLA is defined as mean −2 × SD. A, top, group A; B, bottom, group B.

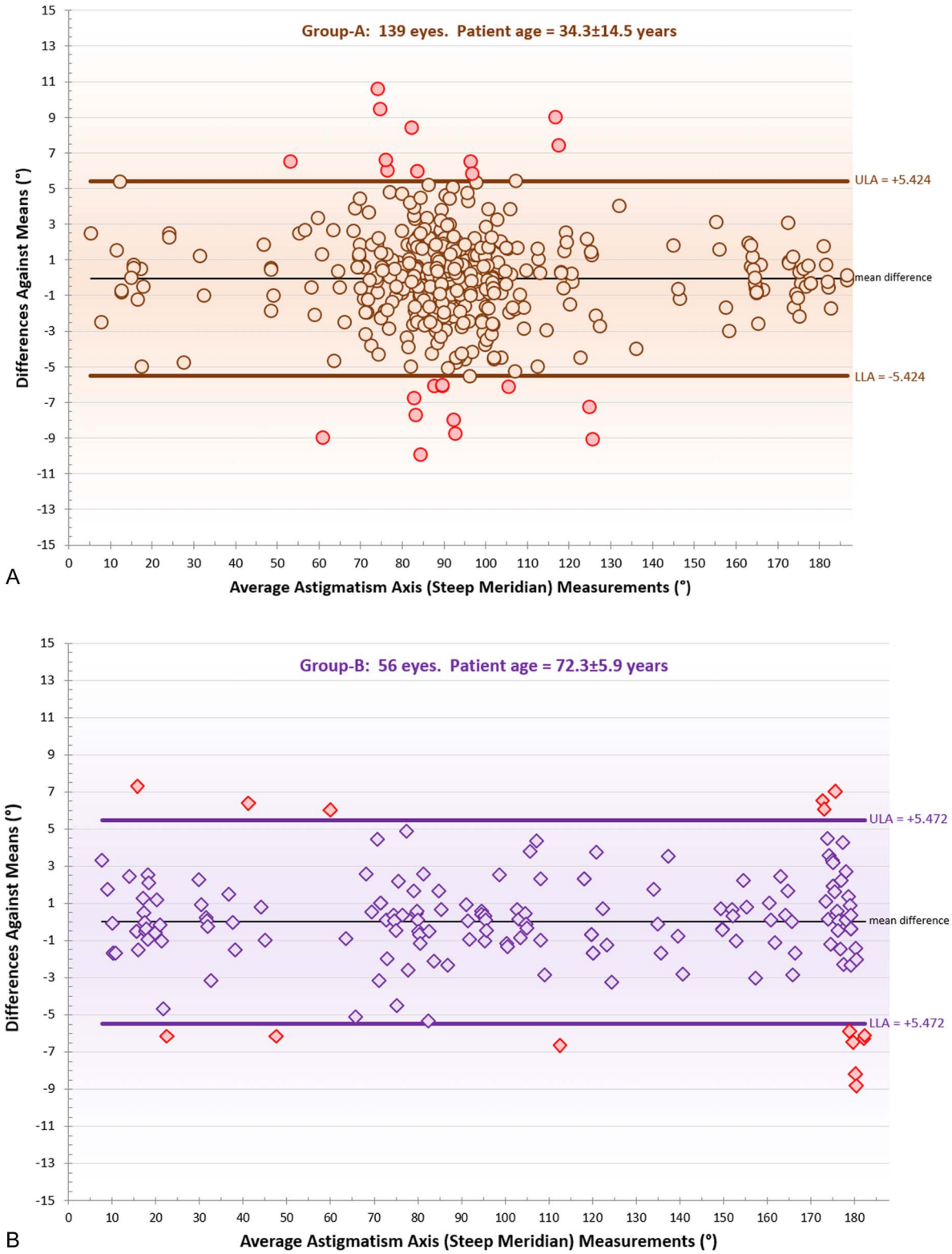

FIGURE 4. Bland–Altman plots illustrating the difference against means versus average astigmatism axis measurements (reported in degrees). The ULA is defined as mean +2 × SD. The LLA is defined as mean −2 × SD. A, top, group A; B, bottom, group B.

Figure 4 presents Bland–Altman plots for astigmatism axis measurements. In group A (Fig. 4A), the coefficient of repeatability was 5.4 degrees whereas in group B (Fig. 4B) 5.5 degrees.

The repeatability of axis measurement had an inverse relationship with the magnitude of astigmatism: the larger the magnitude, the smaller the repeatability of axis measurement. However, there was no clear relationship between the repeatability of the magnitude of astigmatism and increasing magnitude of astigmatism in either group (Tables 1 and 2). We further explored the possible correlation between the repeatability of axis measurement and magnitude of astigmatism. The linear fit regression curve had a coefficient of linearity $r^2 = 0.4$; the negative slope indicated that in every ~1-D increase of the astigmatism magnitude, there was approximately a 0.4 degree reduction (improvement) in axis measurement repeatability. As shown in the results listed in Tables 1 and 2, within the 0.0-to-1.0 D subgroups of astigmatism, the axis measurement repeatability was on average 6.2 and 5.3 degrees (groups A and B, respectively); in the subgroups 1.0 to 3.0 D, 3.0 and 2.2 degrees; in the subgroups 3.0 to 6.0 D, 1.4 and 1.2 degrees; and in the subgroups of astigmatism larger than 6.0 D, 1.1 and 0.6 degrees.

TABLE 2. Repeatability of Astigmatism Magnitude (D) and Axis (Degrees) Measurements Versus the Amount of Astigmatism (D) in the 4 Stratified Subgroups of Precataract Patients Forming Group B

Astigmatism Subgroups (Range in D)		Magnitude Repeatability (D)	Axis Repeatability (Degrees)	Average Astigmatism (D)
0.0 to 1.0	Mean	0.4	5.8	0.6
n = 28	SD	±0.4	±2.6	±0.2
	Minimum	0.1	0.5	0.1
	Maximum	0.8	8.6	1.0
1.0 to 3.0	Mean	0.4	2.2	1.3
n = 15	SD	±0.5	±2.2	±0.2
	Minimum	0.0	0.2	1.0
	Maximum	0.8	4.9	2.8
3.0 to 6.0	Mean	0.4	1.2	3.6
n = 9	SD	±0.4	±0.8	±0.3
	Minimum	0.0	0.4	3.0
	Maximum	0.5	2.4	5.9
>6.0	Mean	0.5	0.6	3.5
n = 4	SD	±0.4	±0.6	±0.4
	Minimum	0.1	0.1	6.1
	Maximum	0.7	1.7	7.9

DISCUSSION

Corneal topography systems have continuously improved over the past 20 years.[11,12] Placido ring topography, evolved as videokeratography,[13] is perhaps the most widespread and established modality. It seems to have currently surpassed manual keratometry in clinical practice for the purpose of astigmatism measurement.[14,15] Among the advantages justifying the widespread acceptance of Placido topography are the noncontact nature and the single-shot capture, which help reduce motion artifacts. However, there are a number of limitations associated with this technique, such as the skew ray error,[16,17] data interpolation at the corneal apex, and susceptibility to error in areas of abrupt corneal elevation changes.[18,19] Numerical algorithms neglect skew ray reflections,[20] leading to inaccuracy in reconstructing nonrotationally symmetric corneas.[21]

TABLE 1. Repeatability of Astigmatism Magnitude (D) and Axis (Degrees) Measurements Versus the Amount of Astigmatism (D) in the 4 Stratified Subgroups of Younger-Age Patients Forming Group A

Astigmatism Subgroups (Range in D)		Magnitude Repeatability (D)	Axis Repeatability (Degrees)	Average Astigmatism (D)
0.0 to 1.0	Mean	0.2	6.2	0.7
n = 83	SD	±0.3	±2.5	±0.2
	Minimum	0.0	0.2	0.2
	Maximum	1.2	11.6	1.0
1.0 to 3.0	Mean	0.3	3.0	1.4
n = 33	SD	±0.4	±1.3	±0.3
	Minimum	0.0	0.2	1.0
	Maximum	1.3	8.2	3.0
3.0 to 6.0	Mean	0.6	1.4	2.4
n = 17	SD	±0.7	±1.0	±0.3
	Minimum	0.0	0.0	3.0
	Maximum	1.0	6.2	6.0
>6.0	Mean	0.4	1.1	4.8
n = 6	SD	±0.5	±0.7	±1.7
	Minimum	0.1	0.1	6.0
	Maximum	0.9	0.8	9.2

Placido-based systems project a pattern of concentric black-and-white rings (mires) on the anterior corneal surface—or more precisely, the air–tear film interface—acting as a convex mirror.[22,23] The captured image of this pattern is analyzed, and on the basis of mire image magnification, the radius of curvature of this "mirror" is calculated; based on specific algorithms and conditions, the refractive power of the corneal surface is also derived. Corneal surface topographic elevation maps are then provided by interpolation and specific surface-fitting protocols.

Corneal surface topographic elevation maps are critical to ensure the most accurate and precise astigmatism measurement.[24] Actual (not interpolated) elevation maps require primary data from 3-dimensional imaging of the corneal contour, in which the elevation of individual corneal surface points is derived from triangulation.[25] Among such rare true elevation-based topography devices has been (no longer commercially available) the PAR Corneal Topographer (PAR CTS; PAR Technology, New Hartford, NY). The system projected on the corneal surface a raster grid pattern, which was captured by an off-axis camera. Highly accurate corneal surface elevation maps were then produced, by analyzing the pattern projections, using raster photogrammetry.[26,27]

The new corneal topography methodology introduced by the Cassini is also a "true" elevation-based system. Each "color-coded" LED point has a unique color combination of

surrounding points, thus enabling a triangulation-based evaluation of the corneal surface. Because of this, the primary maps offered by this device are based on true elevation differentials.

This work, using the Cassini topographer, confirms corneal astigmatism distribution in regard to with-the-rule and against-the-rule distributions[28] and their changing nature with age, that is, the shift of the astigmatism axis with age.[29] Specifically, the distribution was found to be predominantly with-the-rule in the younger population and against-the-rule within the older population.

The distribution of the astigmatism magnitude reported in this study is in agreement with those reported in previous studies. In a recent large study of 1230 eyes with a mean patient age of 75.5 ± 10.7 years,[30] in 79.5% of eyes, the corneal astigmatism was 1.5 D or less; in 9.7%, >2.0 D; in 4.6%, >2.5 D; in 1.9%, 3.0 D or more; and in 1.0%, >3.5 D. Other publications[31] report that >40% of the examined eyes had astigmatism larger than 1.0 D, and others report about a quarter of the eyes with astigmatism >1.5 D.[32] In this study, we observed that astigmatism ≥1.0 D was noted in approximately 60% of the younger-age population (group A) and in 50% of the precataract population (group B).

In this study, the repeatability of astigmatism measurement in both groups was on average <0.4 D. These data compare better than literature-reported values of keratometry repeatability measured by established corneal evaluation devices such as manual keratometry,[33,34] Placido topography,[35] slit-scan (Orbscan II; Bausch & Lomb, Rochester, NY), Scheimpflug imaging using devices such as the Pentacam (Oculus, Wetzlar, Germany), the Galilei (Ziemer Ophthalmic Systems AG, Switzerland),[36] and the Sirius (CSO Costruzione Strumenti Oftalmici, Scandicci Firenze, Italy).[37] For example, the SD of the corneal astigmatism magnitude measured by automated keratometry measurements was ±0.3 D (thus the repeatability was 0.6 D).[38]

We noted in this study an improvement of repeatability of axis measurement with increasing magnitude of astigmatism. Particularly important is the finding that in the "large" astigmatism subgroups, the repeatability of axis measurement ranged from 1.4 degrees (younger patients) to 1.2 degrees (older, precataract patients) within the subgroups with astigmatism 3.0 to 6.0 D, and from 1.1 degrees (younger patients) to 0.6 degrees (older, precataract patients) within the subgroups with astigmatism larger than 6.0 D. These repeatability values compare well with those reported in the peer-reviewed literature: a study reported an axis within 5 degrees in 72.1% of eyes,[39] whereas another study comparing the autokeratometer and the Placido corneal topographer found limits of agreement between −15.3 and 17.5 degrees for axis measurement[40] (thus the repeatability was 16.4 degrees).

These findings of improved axis measurement repeatability may bear clinical value, considering the possibility of using the Cassini for axis determination in cataract surgery in which toric intraocular lenses (IOLs) will be used. Additionally, improved keratometry repeatability measurement may contribute to more predictable IOL power calculation. The repeatability study in this work relates directly to the precision of measurement of corneal astigmatism. Device accuracy (not examined in this study) may be further evaluated with calibration targets graduated with interferometry standards, or by comparison with other videokeratographers that have already been assessed for accuracy.

Clinical Significance

Cataract surgery, although initially used to remove the opaque crystalline lens, has recently been increasingly evaluated in regard to its optimal refractive outcome that may significantly affect the quality of everyday life. Patients and clinicians' expectations dictate the least amount of postoperative astigmatism and sphere. Effective correction of astigmatism, using toric IOLs and/or astigmatic keratotomy, poses additional high standards in assessing the exact amount and axis of clinical astigmatism. Key requirement for this purpose is the precise and accurate measurement of the value and axis of the preoperative corneal astigmatism.[41]

Achieving emmetropia in cataract surgery relies on accurate and precise axial length measurement (by ×2.5 fold according to the Sanders, Retzlaff, and Kraft formula) as well as on keratometry measurement (by ×0.9 fold). Axial length measurements have reached high levels of accuracy and precision with the use of partial coherence interferometry-based biometry devices that may offer predictable measurements to the hundredth of a millimeter.[42] Considering the measurement of axial length variable quite predictable, keratometry measurement becomes an equally significant variable in precataract surgery biometry, especially considering that keratometry deriving from corneal topography has an "accepted" SD of 1 D, which translates to a possible error of approximately 1 D in IOL power calculations.

In contrast, refractive surgery has employed internationally for many years corneal topography data in topography-guided treatments aiming to correct corneal irregularities or even improve refractive outcomes in routine myopic, hyperopic, and/or astigmatic eyes by improving corneal symmetry.[43–45] We have previously reported the use of topography and tomography and also compared corneal imaging devices for topography-guided refractive and therapeutic interventions with an excimer laser.[46] We have also recently reported the use of corneal topography in applying topography-guided variable fluence collagen cross-linking.[47]

An additional clinical utility of the data presented in this study may be found in cases in which Placido reflection topography data do not coincide with Scheimpflug type–derived tomography, in which case the clinician is compelled to choose a therapeutic topography-guided intervention based on the most objective imaging.

CONCLUSIONS

Astigmatism seems to shift from on average with-the-rule to against-the-rule with aging. The use of this alternative multicolored LED spot reflection topography further improves astigmatism magnitude repeatability and axis repeatability. This enhanced precision may find further applications in clinical diagnostics, and possibly intraoperative topography-guidance both in cataract and in refractive surgery.

REFERENCES

1. Rand RH, Howland HC, Applegate RA. Mathematical model of a Placido disk keratometer and its implications for recovery of corneal topography. *Optom Vis Sci.* 1997;74:926–930.
2. Vos FM, van der Heijde RGL, Spoelder HJW, et al. A new instrument to measure the shape of the cornea based on pseudorandom color coding. *IEEE Trans Instrum Meas.* 1997;46:794–797.
3. Snellenburg JJ, Braaf B, Hermans EA, et al. Forward ray tracing for image projection prediction and surface reconstruction in the evaluation of corneal topography systems. *Opt Express.* 2010;18:19324–19338.
4. Sicam VA, Snellenburg JJ, van der Heijde RG, et al. Pseudo forward ray-tracing: a new method for surface validation in cornea topography. *Optom Vis Sci.* 2007;84:915–923.
5. Sicam VA, van der Heijde RG. Topographer reconstruction of the nonrotation-symmetric anterior corneal surface features. *Optom Vis Sci.* 2006;83:910–918.
6. Kanellopoulos AJ, Asimellis G. Clinical correlation between placido, scheimpflug and LED color reflection topographies in imaging of a scarred cornea. *Case Rep Ophthalmol.* 2014;5:311–317.
7. Kanellopoulos AJ, Asimellis G. Forme fruste keratoconus imaging and validation via point-source reflection topography. *Case Rep Ophthalmol.* 2013;4:199–209.
8. Chylack LT Jr, Wolfe JK, Singer DM, et al. The lens opacities classification system III. *Arch Ophthalmol.* 1993;111:831–836.
9. Gupta M, Ram J, Jain A, et al. Correlation of nuclear density using the Lens Opacity Classification System III versus Scheimpflug imaging with phacoemulsification parameters. *J Cataract Refract Surg.* 2013;39: 1818–1823.
10. Smolek MK, Klyce SD. Current keratoconus detection methods compared with a neural network approach. *Invest Ophthalmol Vis Sci.* 1997; 38:2290–2299.
11. Maguire LJ, Singer DE, Klyce SD. Graphic presentation of computer-analyzed keratoscope photographs. *Arch Ophthalmol.* 1987;105: 223–230.
12. Koch DD, Foulks GN, Moran CT, et al. The Corneal EyeSys System: accuracy analysis and reproducibility of first-generation prototype. *Refract Corneal Surg.* 1989;5:424–429.
13. Read SA, Collins MJ, Iskander DR, et al. Corneal topography with Scheimpflug imaging and videokeratography: comparative study of normal eyes. *J Cataract Refract Surg.* 2009;35:1072–1081.
14. Koch DD, Haft EA. Introduction to corneal topography. In: Gills JP, Sanders DR, Thornton SP, et al, eds. *Corneal Topography: The State of the Art*. Thorofare, NJ: SLACK Inc; 1995:3–15.
15. Tripoli NK, Cohen KL, Obla P, et al. Height measurement of astigmatic test surfaces by a keratoscope that uses plane geometry surface reconstruction. *Am J Ophthalmol.* 1996;121:668–676.
16. Klein SA. Axial curvature and the skew ray error in corneal topography. *Optom Vis Sci.* 1997;74:931–944.
17. Iskander DR, Davis BA, Collins MJ. The skew ray ambiguity in the analysis of videokeratoscopic data. *Optom Vis Sci.* 2007;84:435–442.
18. Klein SA. Corneal topography reconstruction algorithm that avoids the skew ray ambiguity and the skew ray error. *Optom Vis Sci.* 1997;74:945–962.
19. Kanellopoulos AJ, Asimellis G. Comparison of Placido disc and Scheimpflug image-derived topography-guided excimer laser surface normalization combined with higher fluence CXL: the Athens Protocol, in progressive keratoconus. *Clin Ophthalmol.* 2013;7:1385–1396.
20. van Saarloos PP, Constable IJ. Improved method for calculation of corneal topography for any photokeratoscope geometry. *Optom Vis Sci.* 1991;68:960–965.
21. Greivenkamp JE, Mellinger MD, Snyder RW, et al. Comparison of three videokeratoscopes in measurement of toric test surfaces. *J Refract Surg.* 1996;12:229–239.
22. Shirayama M, Wang L, Weikert MP, et al. Comparison of corneal powers obtained from 4 different devices. *Am J Ophthalmol.* 2009;148: 528–535.e1.
23. Mejía-Barbosa Y, Malacara-Hernández D. A review of methods for measuring corneal topography. *Optom Vis Sci.* 2001;78:240–253.
24. Belin MW, Khachikian SS. An introduction to understanding elevation-based topography: how elevation data are displayed–a review. *Clin Exp Ophthalmol.* 2009;37:14–29.
25. Ambrósio R Jr, Belin MW. Imaging of the cornea: topography vs tomography. *J Refract Surg.* 2010;26:847–849.
26. Belin MW. Intraoperative raster photogrammetry–the PAR corneal topography system. *J Cataract Refract Surg.* 1993;19(suppl):188–192.
27. Belin MW, Litoff D, Strods SJ, et al. The PAR technology corneal topography system. *Refract Corneal Surg.* 1992;8:88–96.
28. Hayashi K, Hayashi H, Hayashi F. Topographic analysis of the changes in corneal shape due to aging. *Cornea*. 1995;14:527–532.
29. Asano K, Nomura H, Iwano M, et al. Relationship between astigmatism and aging in middle-aged and elderly Japanese. *Jpn J Ophthalmol.* 2005; 49:127–133.
30. Khan MI, Muhtaseb M. Prevalence of corneal astigmatism in patients having routine cataract surgery at a teaching hospital in the United Kingdom. *J Cataract Refract Surg.* 2011;37:1751–1755.
31. Ferrer-Blasco T, Montés-Micó R, Peixoto-de-Matos SC, et al. Prevalence of corneal astigmatism before cataract surgery. *J Cataract Refract Surg.* 2009;35:70–75.
32. Hoffer KJ. Biometry of 7,500 cataractous eyes. *Am J Ophthalmol.* 1980; 90:360–368.
33. Karabatsas CH, Cook SD, Papaefthymiou J, et al. Clinical evaluation of keratometry and computerised videokeratography: intraobserver and interobserver variability on normal and astigmatic corneas. *Br J Ophthalmol.* 1998;82:637–642.
34. Visser N, Berendschot TT, Verbakel F, et al. Comparability and repeatability of corneal astigmatism measurements using different measurement technologies. *J Cataract Refract Surg.* 2012;38: 1764–1770.
35. Karabatsas CH, Papaefthymiou I, Aslanides IM, et al. Comparison of keratometric and topographic cylinder and axis measurements on normal corneas with low astigmatism. *Eur J Ophthalmol.* 2005;15:8–16.
36. Crawford AZ, Patel DV, McGhee CN. Comparison and repeatability of keratometric and corneal power measurements obtained by Orbscan II, Pentacam, and Galilei corneal tomography systems. *Am J Ophthalmol.* 2013;156:53–60.
37. De la Parra-Colín P, Garza-León M, Barrientos-Gutierrez T. Repeatability and comparability of anterior segment biometry obtained by the Sirius and the Pentacam analyzers. *Int Ophthalmol.* 2014;34:27–33.
38. Ninomiy Y, Kanazawa Y, Kojima Y, et al. Simulation of toric intraocular lens results: the effect of repeatability and increments of automated keratometry [in Japanese] *Nihon Ganka Gakkai Zasshi.* 2013;117: 621–628.
39. Bullimore MA, Buehren T, Bissmann W. Agreement between a partial coherence interferometer and 2 manual keratometers. *J Cataract Refract Surg.* 2013;39:1550–1560.
40. Kobashi H, Kamiya K, Igarashi A, et al. Comparison of corneal power, corneal astigmatism, and axis location in normal eyes obtained from an autokeratometer and a corneal topographer. *J Cataract Refract Surg.* 2012;38:648–654.
41. Dupps WJ Jr. Astigmatic correction in cataract surgery: lens or cornea? *J Cataract Refract Surg.* 2014;40:1577–1578.
42. Kaswin G, Rousseau A, Mgarrech M, et al. Biometry and intraocular lens power calculation results with a new optical biometry device: comparison with the gold standard. *J Cataract Refract Surg.* 2014;40:593–600.
43. Kanellopoulos AJ, Kahn J. Topography-guided hyperopic LASIK with and without high irradiance collagen cross-linking: initial comparative clinical findings in a contralateral eye study of 34 consecutive patients. *J Refract Surg.* 2012;28(11 suppl):S837–S840.
44. Basmak H, Sahin A, Yildirim N, et al. Measurement of angle kappa with synoptophore and Orbscan II in a normal population. *J Refract Surg.* 2007;23:456–460.
45. Kanellopoulos AJ, Pe LH. Wavefront-guided enhancements using the wavelight excimer laser in symptomatic eyes previously treated with LASIK. *J Refract Surg.* 2006;22:345–349.
46. Kanellopoulos AJ. Topography-guided hyperopic and hyperopic astigmatism femtosecond laser-assisted LASIK: long-term experience with the 400 Hz eye-Q excimer platform. *Clin Ophthalmol.* 2012;6:895–901.
47. Kanellopoulos AJ, Asimellis G. Hyperopic correction: clinical validation with epithelium-on and epithelium-off protocols, using variable fluence and topographically customized collagen corneal cross-linking. *Clin Ophthalmol.* 2014;8:2425–2433.